Proc. Natl. Acad. Sci. USA
Vol. 87, pp. 4895–4899, July 1990
Microbiology

Multiple-exposure photographic analysis of a motile spirochete

(motility/periplasmic flagella/*Leptospiraceae*)

STUART F. GOLDSTEIN*† AND NYLES W. CHARON‡

*Department of Genetics and Cell Biology, University of Minnesota, Saint Paul, MN 55108; and ‡Department of Microbiology and Immunology, West Virginia University, Health Sciences Center, Morgantown, WV 26506

Communicated by Howard C. Berg, March 26, 1990 (received for review December 18, 1989)

ABSTRACT **The *Leptospiraceae* are thin spirochetes with a unique mode of motility. These spiral-shaped bacteria have internal periplasmic flagella that propel the cells in low-viscosity and gel-like high-viscosity media. A model of *Leptospiraceae* motility has been previously proposed that states that the subterminally attached periplasmic flagella rotate between the outer sheath and the helical protoplasmic cylinder. The shape of the cell ends and the direction of gyration of these ends are determined by the direction of rotation of the internal periplasmic flagella. Rotation of the periplasmic flagella in one direction causes that end to be spiral-shaped, and rotation in the other direction causes that end to be hook-shaped. One prediction of the model is that these right-handed spirochetes roll clockwise when swimming away from an observer. For maximum swimming efficiency, the model predicts that the sense of the spiral-shaped end is left-handed and gyrates counterclockwise. The present study presents direct evidence that the cell rolls clockwise (protoplasmic cylinder helix diameter = 0.24 μm; pitch = 0.69 μm), the ends gyrate counterclockwise, and the spiral-shaped end is left-handed (helix diameter = 0.6 μm; pitch = 2.7 μm)—as predicted by the model. The hook-shaped end appears approximately planar. The approach used was to illuminate stroboscopically cells slowed by Ficoll and analyze the resultant multiple-exposure photographs focused above and below the axis of the cell. The methodology used should be helpful in analyzing the motility of the larger and more complex spirochetes.**

The *Leptospiraceae* are thin spiral (i.e., helical)-shaped bacteria with a diameter of 0.1–0.2 μm and a length of 6–20 μm (1–6). At present, the family consists of three species: *Leptospira biflexa*, *Leptospira interrogans*, and *Leptonema illini* (3, 7). All three species have a similar morphology: each species has internal periplasmic flagella (PFs, also termed axial filaments or endoflagella) located between an outer membrane sheath and a right-handed helically shaped protoplasmic cylinder (PC) (1–6, 8–10). The PC is helical over the entire length of the cell (8). A single PF is attached subterminally at each end and extends toward the center; these PFs do not overlap in the center (5, 6, 11). Electron microscopy has revealed that the PFs of *Leptospiraceae* (1, 4) are structurally similar to those of rod-shaped bacteria, with a filament, hook-region, and basal discs (12). Genetic evidence strongly suggests that these PFs are involved in motility (11).

The *Leptospiraceae* exhibit a number of different cell shapes when swimming. In cells that are translating through the medium, the anterior end is helical or spiral (S)-shaped and the posterior end is hook (H)-shaped (Fig. 1*c*) (2, 13–19). The pitch and helix diameter (defined in Fig. 2) of the S-shaped end are larger than those of the PC helix. Nontranslating forms are also seen; both ends of these cells are either H-shaped or both ends are S-shaped (Fig. 1 *a* and *b*) (15, 17–19). Cells readily change from one form to the other.

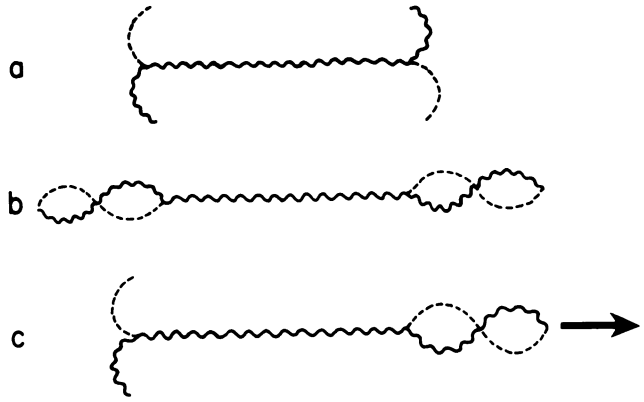

FIG. 1. Movement of *L. illini* in liquid medium. (*a* and *b*) Nontranslational forms referred to as the H–H (*a*) or S–S (*b*) configurations. Translating cells (*c*) are in the H–S, or S–H configurations. The arrow points toward the direction of swimming. Reproduced with permission from ref. 17 (copyright American Society for Microbiology).

Berg *et al.* (17) have proposed a model for *Leptospiraceae* motility. This model is based on an analysis of motility mutants of *L. illini*, which have altered PFs (11). The model states that the PFs propel the organisms by rotation in a manner analogous to flagellar rotation in rod-shaped bacteria (12, 20). In addition, the shapes of the cell ends are determined by the shapes of the PFs, which are in part determined by their direction of rotation. Rotation of a PF in one direction causes that end to be S-shaped, and rotation in the opposite direction results in that end being H-shaped. Two sources of forward thrust have been proposed (17). (*i*) Rotation of the anterior PF causes that end of the cell to gyrate. [By "gyrate" we mean that each point moves in a circular path about the cell axis, without reference to whether or not points on the surface rotate, in analogy to the laterally bending rubber tube with an internally rotating bent wire as diagrammed by Taylor (21).] This gyration generates a backward-moving spiral wave. It is this spiral wave that propels the cell in low-viscosity medium. (*ii*) The other source of thrust is the rolling of the PC helix around the PFs. It is this motion that allows the spirochetes to swim through gel-like medium, such as methylcellulose, without slippage. Both motions occur together: the PF rotates in one direction, and the cell cylinder rolls in the opposite direction.

The various forms of motile cells (Fig. 1) can be explained by the model (17). As viewed from one end of the cell toward the other end, nontranslating cells have their PFs rotating in opposite directions, and translating cells have their PFs

The publication costs of this article were defrayed in part by page charge payment. This article must therefore be hereby marked "*advertisement*" in accordance with 18 U.S.C. §1734 solely to indicate this fact.

Abbreviations: PF, periplasmic flagellum; S, spiral; H, hook; CW, clockwise; CCW, counterclockwise; PC, protoplasmic cylinder.

†To whom reprint requests should be addressed.

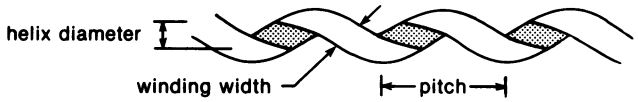

FIG. 2. Diagram of a right-handed helix, showing the helix diameter, pitch, and width of a winding.

rotating in the same direction. This model states that, for maximum swimming efficiency, the helical sense (right handed or left handed) of an S-shaped end should be opposite to that of the PC helix. [We adopt the frame of reference of viewing the cell from the posterior end toward the anterior end; a right-handed helix spirals clockwise (CW) moving away from an observer, and a left-handed helix spirals counterclockwise (CCW) moving away from an observer.] An analysis of the PC helix of these spirochetes has since shown that they are right-handed (8–10). This implies that as the PC rolls CW, the S- and H-shaped ends should gyrate CCW. In addition, the S-shaped end should be left-handed. This and other models of spirochete motility have been reviewed (19).

Indirect evidence that the S- and H-shaped ends gyrate as predicted by the model of Berg *et al.* (17) has been obtained from an analysis of tethered cells of *L. illini* (18). In the present study, direct evidence was found that the ends do indeed gyrate as predicted by this model. In addition, the results indicate that the S-shaped end is left-handed, and the H-shaped end appears approximately planar. Cells were illuminated stroboscopically for viewing and multiple-exposure photography. Analyses of cell shapes and motions were facilitated by focusing above and below the axis of the cells (22, 23) and by slowing the motions of the cells by suspending them in Ficoll (24).

EXPERIMENTAL PROCEDURES

Cell Preparation and Microscopy. Cells of *L. illini* were grown and maintained in EMJH medium as described (8, 11). The temperature for all observations was 20°C. A basal suspending solution containing 20 mM NaCl, 0.1 mM $CaCl_2$, 0.05 mM $MgSO_4$, 7 mM Na_2HPO_4, 2.2 mM KH_2PO_4, and 1% bovine serum albumin (pH 7.4) was used for most observations and photography. For most direct observations and photography, the basal medium was supplemented to a final concentration of 31.5% (wt/vol) Ficoll (M_r = 400,000) (Sigma). The viscosity of the bovine serum albumin/Ficoll medium was 65 cP (0.065 $N \cdot s \cdot m^{-2}$) as determined using a Cannon–Fenske viscometer. For nonslip swimming, the Ficoll was replaced with 1% methylcellulose (2% = 4 $N \cdot s \cdot m^{-2}$ = 4000 cP, Matheson).

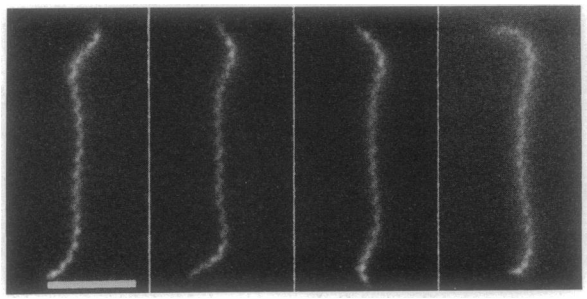

FIG. 3. Transition from an S- to an H-shaped end. The transition can be seen between the second and third exposures. The focus is above the cell and regions in focus appear brightest. (Bar = 5 μm.) In all multiple-exposure photographs, the first image is on the left and the time between exposures = 0.1 s.

To view the cells, a drop of the Ficoll or methylcellulose solution was placed on a slide, and a loop of cells in culture medium was placed on this drop. The drop was then stirred gently with a toothpick and covered by a cover glass that was supported on its edges by a mixture of 3 parts Vaseline to 1 part paraffin. A Tiyoda oil-immersion toroidal condenser (Technical Instruments, San Francisco) was used with a Zeiss WL microscope. Stroboscopic illumination was provided by a modified Chadwick–Helmuth power supply and xenon lamp (Chadwick–Helmuth, Monrovia, CA) (25, 26). Cell motions were slow enough not to be confused with stroboscopic effects. Because these cells are immobilized by strong blue light (18, 27, 28), observations were made at low-light intensities, usually using a yellow–green filter.

Photomicroscopy. All photographs were taken on Kodak Tri-X film and developed in Acufine (Chicago). Multiple-image photographs were taken with the film moving (25, 26) with illumination at 10 flashes per s. A Zeiss motor-driven 35-mm camera was modified to allow adjustment of the speed of advancement of the film. An ×100 planachromat objective, ×8 ocular, and ×0.5 reflex adapter were used and produced a magnification of ×400 on the film. The iris diaphragm of the objective was adjusted to the maximum aperture that prevented excessive background illumination, which was approximately 1.0. As determined using a stage micrometer, the images were not reversed either through the viewing oculars or on film.

For photography, the camera was started, the shutter was opened, the filter was removed, and the light intensity was

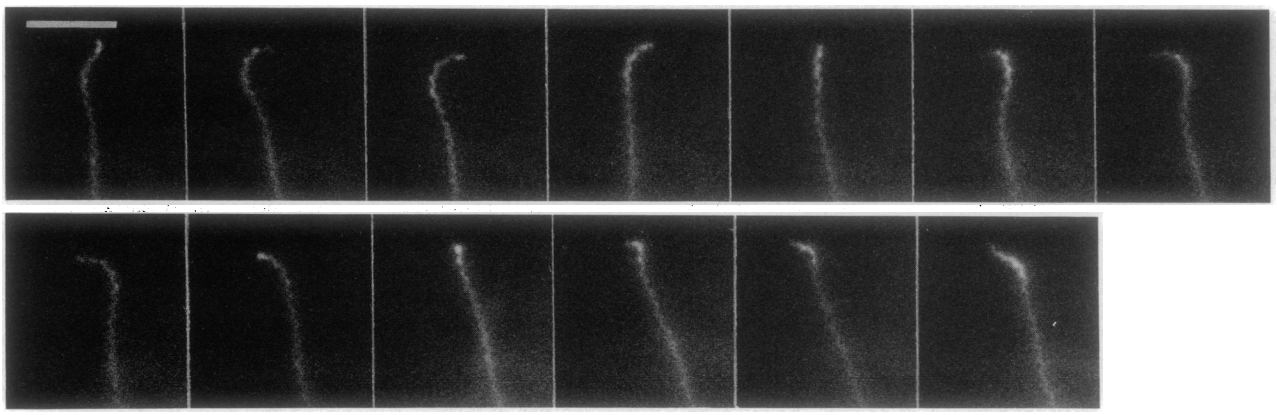

FIG. 4. Transition between H- and S-shaped ends and gyration of the H-shaped end. A transition from S to H can be seen between the 1st and 2nd exposures, and a transition from H to S can be seen between the 10th and 11th exposures. The H-shaped end appears to gyrate from right to left when it is above the helix axis in the 3rd to 10th exposures, indicating a CCW gyration when viewed from behind the cell (i.e., from top of photograph). See Fig. 3.

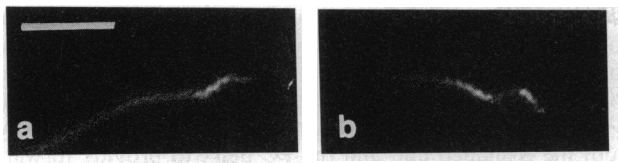

FIG. 5. Left-handed sense of S-shaped end. (*a*) Focused above the helix axis. (*b*) Focused below the helix axis. See Fig. 3.

increased to 7.5 J per flash. Cells were checked after being photographed to verify that they were still swimming. Measurements of the pitch and helix diameter of S-shaped ends were made on prints at a magnification of ×6000; for most cells, two images, with the ends about 180° out of phase with one another, were measured. Because these helices were not long enough to measure their complete pitch, the pitch was taken as twice the distance between two adjacent peaks, measured parallel to the cell axis (Fig. 2). For measurement of PC helices, photographs of light-immobilized cells were made with the film stationary. Measurements of PCs were made on prints at a magnification of ×7500. Pitches were determined from the distance spanned by 20 peaks. Because the location of the body axis was difficult to estimate in images of the PC helix, the helix diameter was taken as the total width of the image of the PC minus the winding width of the image (see Fig. 2). Parameters calculated include pitch angle = arctan [pitch/(π × helix diameter)], radius of curvature = helix diameter/[2 $\cos^2$(pitch angle)], and length/period = [(π × helix diameter)^2 + (pitch)^2]$^{1/2}$. Photographs of nonslip swim paths in methylcellulose were taken with the film stationary at 45 flashes per s (cf. ref. 29).

RESULTS

Motion of Swimming Cells in Ficoll. Advancing cells exhibited an anterior S-shape and a posterior H-shape, and nonadvancing cells had either both ends S-shaped or both ends H-shaped (2, 13–19). Cells were observed at various phases of the culture cycle; no major differences were noted in waveforms. S-shaped ends typically gyrated several turns per second in Ficoll, and cells made little forward advancement in this solution (24). As can be seen in Figs. 3 and 4, transitions between S- and H-shapes occurred within 0.1 s.

Analysis of S-Shaped Ends. As can be seen in Figs. 3–6, the overall morphology of the S-shaped ends can be clearly discerned. These ends had a helix diameter of 0.6 ± 0.1 μm and a pitch of 2.7 ± 0.5 μm (mean ± SD, n = 17 cells). Measurements of helix diameter and pitch indicate a pitch angle = 0.97 ± 0.10 radian, a radius of curvature = 1.0 ± 0.3 μm, and a length/period = 3.3 ± 0.4 μm. S-shaped ends do not appear to be perfect circular helices. Perfectly helical ends should appear sinusoidal in cells swimming parallel to the cover glass; they should appear more rounded in cells swimming obliquely to the cover glass. However, as can be seen in Figs. 3–6, S-shaped ends often appear to have straighter sides and more angular peaks than sine waves. S-shaped ends appear to be about one period long in the photographs, but they do not bend sharply enough at their proximal ends to determine their length precisely. No appreciable effects were noted with respect to the influence of an S or H shape at one end upon the exact shape at the other end.

Direct evidence was obtained that the S-shaped end is left-handed and gyrates CCW. In cells swimming parallel to the cover glass, the sense of winding of a helix—right-handed or left-handed—can be surmised from the direction of slant of portions of the cell in photographs focused above or below the helix axis (22, 23). As shown in Fig. 5*a*, portions of the S-shaped end above the axis slant from lower left to upper right when the cell axis is horizontal in the photograph. As can be seen in Fig. 5*b*, portions of the S-shaped end below the helix axis slant from upper left to lower right. These results indicate that the S-shaped end is left-handed. As S-shaped ends gyrated, successively more posterior points passed through the focal plane, as shown in Fig. 6. The result is the familiar barber-pole illusion that the helix is moving toward the opposite end of the cell. This apparent backward motion of a left-handed helix strongly indicates that the S-shaped end is gyrating CCW.

Analysis of H-Shaped Ends. As can be seen in Figs. 3 and 4, the H-shaped ends appear approximately planar. Their radii appear to be constant over their length or to decrease with distance from the end of the cell. By focusing above or below the cell, the direction of gyration of the H-shaped end was determined. As can be seen in Fig. 4, focused above the cell axis, successive frames indicate that the H-shaped ends gyrate CCW.

Analysis of the PC. The general morphology of the protoplasmic cylinder was analyzed. The PC helix is shown in Fig. 7, with the plane of focus above, in, or below the helix axis. Portions of the PC helices above and below the helix axis slanted in directions opposite to those of the S-shaped ends, indicating that the PC helices are right-handed. These observations are in agreement with those of scanning electron microscopic studies (8–10). The helix diameter was 0.24 ±

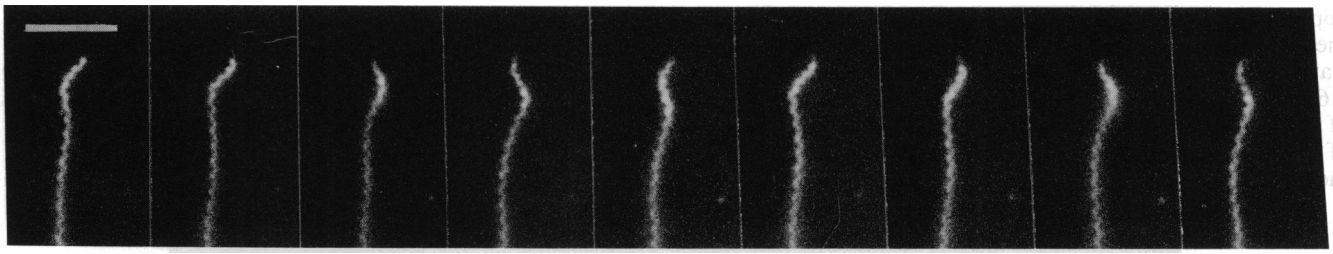

FIG. 6. Gyration of S-shaped end. Oblique regions of the S-shaped end can be seen to progress away from the anterior end (i.e., away from top of photograph), indicating CCW gyration as seen from behind the cell (i.e., from bottom of photograph). See Fig. 3.

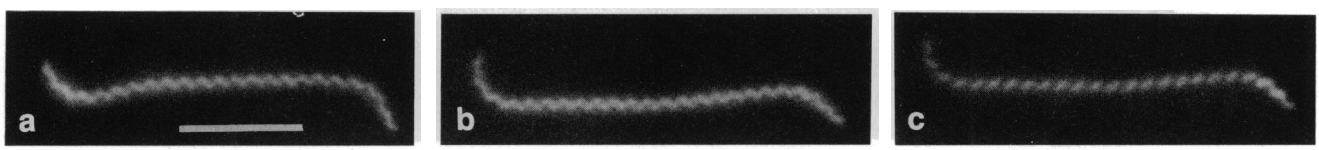

FIG. 7. Right-handed sense of PC helix. (*a*) Focused above helix axis. (*b*) Focused on helix axis. (*c*) Focused below helix axis. See Fig. 3.

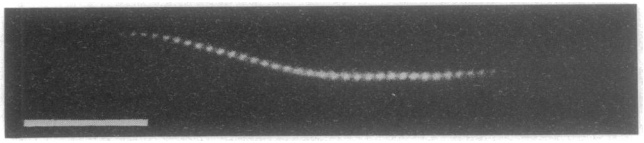

FIG. 8. Multiple-exposure photograph of a swimming cell in 1% methylcellulose illustrating no slippage of the PC helix. Shutter was open for approximately 4 s. See Fig. 3.

0.05 μm and the pitch was 0.69 ± 0.04 μm (n = 14 cells). Similar results have been reported using transmission electron microscopy (30).

The shape and direction of rolling of the PC helix were determined in swimming cells. We find by direct observation that the cells have right-handed helices as they swim in both Ficoll and methylcellulose (data not shown). As shown in Fig. 8, and in agreement with previous results, cells swam without slippage of the PC helix in 1% methylcellulose (17, 24). In contrast, S–H shaped cells in Ficoll show substantial slip and little advancement; direct observations indicate that the PC exhibits a barber-pole illusion of movement of its right-handed helical windings toward the H-shaped end. This barber-pole movement stops when both ends become S-shaped or H-shaped (data not shown). The results with both methylcellulose and Ficoll indicate that, since the PC helix is right-handed even in swimming cells, the cell rolls in a CW direction during translation. The portion of the PC between the S- or H-shaped ends appeared to be quite flexible. Fig. 9 is a photograph of a cell with two gyrating H-shaped ends. The mid-region of the cell is relatively straight when the H-shaped ends point in opposite directions and curved when the H-shaped ends point in the same direction. The same effect can be seen in the sketches of figure 3 in ref. 2.

DISCUSSION

The results presented here support the model of *Leptospiraceae* motility as proposed by Berg *et al.* (17). (*i*) Direct observations of the S-shaped end of *L. illini* indicate that it is a left-handed helix and that both the S- and H-shaped ends gyrate CCW when viewed from behind the cell. (*ii*) The PC helix is clearly right-handed even in swimming cells: we observe this by direct darkfield microscopy of immobilized cells and of cells swimming in methylcellulose and Ficoll; others find this by scanning electron microscopy (8–10). (*iii*) Because the cell advances without slippage in a gel-like medium (14–17, 24), the PC helix must roll CW. In addition, the right-handed helical windings of the PC of translating cells appear to move toward the H-shaped end in a pure liquid; these results also suggest that the cell rolls CW during translation. Our results differ from those of Cox and Twigg (16), who suggest that swimming cells advance with no rolling of the cell cylinder. Thus the results indicate that the PC helix of translating cells rolls CW and in the opposite direction to the gyrations of the S- and H-shaped ends.

The combination of helical senses and gyration directions found in *L. illini* were predicted as an efficient way of balancing torques and producing forward thrust (17). CW rolling of the PC helix provides counter-torque for the CCW gyration of the S- and H- shaped ends, and their opposing helical senses allow both the S-shaped end and the PC helix to provide forward thrust. It should be noted, however, that there is no direct evidence concerning the direction of rotation of the PFs or outer sheath within these regions of the cell.

The direction of gyration of the cell ends changes as they switch between S- and H-shaped. These results are consistent with the proposal (17) that the PFs cause the end of the cells to assume S- and H-shaped forms as the PFs rotate either CCW or CW, respectively. The change from S to H occurs within 0.1 s in *L. illini*. An analysis of tethered cells indicates that this change occurs within 0.05 s (18). In light-immobilized cells or dead cells (11, 17), both ends resemble the H-shaped ends of motile cells. The PFs, therefore, appear to be H-shaped except when gyrating CCW. In motile cells, the H-shaped ends do gyrate and are not the result of the PF at that end being stopped. Similar results were suggested by the analysis of tethered cells in the H–H configuration (18). Berg *et al.* (17) suggested that the PC is more flexible than the PFs, so that the ends conform to the S- and H-shapes that are thought to be due to the PFs. In the present study, the curvature of the mid-region of the PC can be seen to change periodically in H–H cells, in a manner suggesting that it is flexible and bending in response to the gyrations of the hooks. However, in contrast to bacterial flagella (31), the PC is still sufficiently stable that it does not change handedness during swimming. We think other spirochetes may be less stable.

S-shaped ends do not appear to form perfect circular helices. The forces acting on the PFs in these cells are not understood, so it is not possible to say whether a PF rotated at its terminal end would be expected to form a perfect helix. Also, the PC may wrap around a PF over part or all of its length, so that the form of an S-shaped end may not precisely reflect the shape of the PF within.

Spirochete motility in general is poorly understood. Genetic evidence has accumulated that the PFs are involved in the motility of a wide variety of spirochetes, including the *Leptospiraceae* (11) and the larger and more complex *Treponema* (32) and *Spirochaeta* (33, 34). Recent work with *Spirochaeta aurantia* indicates that individual cells respond to chemoattractants in a temporal gradient (35, 36) and, in contrast to *Escherichia coli* (37), a membrane potential is involved in the signaling process (38). These spirochetes are believed to swim in a manner somewhat different than the one proposed for the *Leptospiraceae* (2, 19, 35, 39). The present study not only yields insight into the mechanism by which the *Leptospiraceae* swim, but presents an approach that should be helpful in analyzing the motility of the more complex spirochetes including the *Treponema*, *Spirochaeta*, and *Borrelia*.

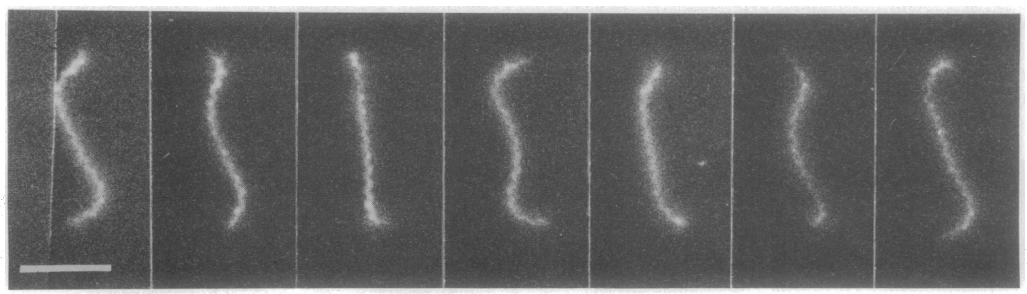

FIG. 9. Bending of PC helix of an H–H-shaped cell, most pronounced in the second, fourth, and sixth exposures. See Fig. 3.

We thank R. C. Johnson and R. F. Bey for their encouragement. This research was supported by Public Health Service Grant DE04645 from the National Institute of Dental Research to N.W.C. and a Grant-in-Aid from the University of Minnesota Graduate School to S.F.G.

1. Holt, S. C. (1978) *Microbiol. Rev.* **42,** 114–160.
2. Canale-Parola, E. (1978) *Annu. Rev. Microbiol.* **32,** 69–99.
3. Johnson, R. C. & Faine, S. (1984) in *Bergey's Manual of Systematic Bacteriology*, eds. Krieg, N. R. & Holt, J. G. (Williams & Wilkins, Baltimore), Vol. 1, pp. 62–67.
4. Nauman, R. K., Holt, S. C. & Cox, C. D. (1969) *J. Bacteriol.* **98,** 264–280.
5. Birch-Andersen, A., Hovind-Hougen, K. & Borg-Petersen, C. (1973) *Acta Pathol. Microbiol. Scand. Sect. B* **81,** 665–676.
6. Hovind-Hougen, K. (1976) *Acta Pathol. Microbiol. Scand. Sect. B. Suppl.* **255,** 1–41.
7. Stallman, N. D. (1987) *Int. J. Syst. Bacteriol.* **37,** 472–473.
8. Carleton, O., Charon, N. W., Allender, P. & O'Brien, S. (1979) *J. Bacteriol.* **137,** 1413–1416.
9. Kayser, A. & Adrian, M. (1978) *Ann. Microbiol. (Paris)* **129A,** 351–360.
10. Yoshii, Z. (1978) *Proc. Jpn. Acad.* **54B,** 200–205.
11. Bromley, D. B. & Charon, N. W. (1979) *J. Bacteriol.* **137,** 1406–1412.
12. Macnab, R. M. (1987) in *Escherichia coli and Salmonella typhimurium: Cellular and Molecular Biology*, eds. Neidhardt, F. C., Ingraham, J. L., Low, K. B., Magasanic, B., Schaecter, M. & Umbarger, H. E. (Am. Soc. Microbiol., Washington), Vol. 1, pp. 70–81.
13. Inada, R., Ido, Y., Hoki, R., Kaneko, R. & Ito, H. (1916) *J. Exp. Med.* **23,** 377–402.
14. Noguchi, H. (1918) *J. Exp. Med.* **27,** 575–592.
15. Jarosch, R. (1967) *Oesterr. Bot. Z.* **114,** 255–306.
16. Cox, P. J. & Twigg, G. I. (1974) *Nature (London)* **250,** 260–261.
17. Berg, H. C., Bromley, D. B. & Charon, N. W. (1978) *Symp. Soc. Gen. Microbiol.* **28,** 285–294.
18. Charon, N. W., Daughtry, G. R., McCuskey, R. S. & Franz, G. N. (1984) *J. Bacteriol.* **160,** 1067–1073.
19. Goldstein, S. F. & Charon, N. W. (1988) *Cell Motil. Cytoskel.* **9,** 101–110.
20. Silverman, M. & Simon, M. (1974) *Nature (London)* **249,** 73–74.
21. Taylor, G. (1952) *Proc. R. Soc. London. Ser. A.* **211,** 225–239.
22. Shimada, K., Kamiya, R. & Asakura, S. (1975) *Nature (London)* **254,** 332–334.
23. Matsuura, S., Kamiya, R. & Asakura, S. (1978) *J. Mol. Biol.* **118,** 431–440.
24. Berg, H. C. & Turner, L. (1979) *Nature (London)* **278,** 349–351.
25. Goldstein, S. F. (1976) *J. Exp. Biol.* **64,** 173–184.
26. Goldstein, S. F. & Schrével, J. (1982) *Cell Motil.* **4,** 369–383.
27. Charon, N. W., Lawrence, C. W. & O'Brien, S. (1981) *Proc. Natl. Acad. Sci. USA* **78,** 7166–7170.
28. Macnab, R. & Koshland, D. E., Jr. (1974) *J. Mol. Biol.* **84,** 399–406.
29. Jahn, T. L. & Landman, M. D. (1965) *Trans. Am. Microsc. Soc.* **84,** 395–406.
30. Hovind-Hougen, K. (1979) *Int. J. Syst. Bacteriol.* **29,** 245–251.
31. Macnab, R. M. & Ornston, M. K. (1977) *J. Mol. Biol.* **112,** 1–30.
32. Limberger, R. J. & Charon, N. W. (1986) *J. Bacteriol.* **166,** 105–112.
33. Paster, B. J. & Canale-Parola, E. (1980) *J. Bacteriol.* **141,** 359–364.
34. Brahamsha, B. & Greenberg, E. P. (1988) *J. Bacteriol.* **170,** 4023–4042.
35. Fosnaugh, K. & Greenberg, E. P. (1988) *J. Bacteriol.* **170,** 1768–1774.
36. Fosnaugh, K. & Greenberg, E. P. (1989) *J. Bacteriol.* **171,** 606–611.
37. Margolin, Y. & Eisenbach, M. (1984) *J. Bacteriol.* **159,** 605–610.
38. Goulbourne, E. A., Jr., & Greenberg, E. P. (1981) *J. Bacteriol.* **148,** 837–844.
39. Berg, H. C. (1976) *J. Theor. Biol.* **56,** 269–273.